Improving satellite-retrieved aerosol microphysical properties using GOCART data

S. Li[1,*], R. Kahn[2], M. Chin[2], M. J. Garay[3], and Y. Liu[1]

[1]Department of Environmental Health, Rollins School of Public Health, Emory University, Atlanta, GA 30322, USA
[2]Laboratory for Atmospheres, NASA Goddard Space Flight Center, Greenbelt, Maryland, USA
[3]Jet Propulsion Laboratory, California Institute of Technology, Pasadena, CA 91109, USA
[*]now at: State Key Laboratory of Remote Sensing Science, Jointly Sponsored by the Institute of Remote Sensing and Digital Earth of CAS and Beijing Normal University, Beijing, 100101, China

Correspondence to: Y. Liu (yang.liu@emory.edu)

Abstract. The Multi-angle Imaging SpectroRadiometer (MISR) aboard the NASA Earth Observing System's Terra satellite can provide more reliable aerosol optical depth (AOD) and better constraints on particle size (Ångström exponent, or ANG), sphericity, and single-scattering albedo (SSA) than many other satellite instruments. However, many aerosol mixtures pass the algorithm acceptance criteria, yielding a poor constraint, when the particle-type information in the MISR radiances is low, typically at low AOD. We investigate adding value to the MISR aerosol product under these conditions by filtering the list of MISR-retrieved mixtures based on agreement between the mixture ANG and absorbing AOD (AAOD) values, and simulated aerosol properties from the Goddard Chemistry Aerosol Radiation and Transport (GOCART) model. MISR–GOCART ANG difference and AAOD ratio thresholds for applying GOCART constraints were determined based on coincident AOD, ANG, and AAOD measurements from the AErosol RObotic NETwork (AERONET). The results were validated by comparing the adjusted MISR aerosol optical properties over the contiguous USA between 2006 and 2009 with additional AERONET data. The correlation coefficient (*r*) between the adjusted MISR ANG derived from this study and AERONET improves to 0.45, compared to 0.29 for the MISR Version 22 standard product. The ratio of the adjusted MISR AAOD to AERONET increases to 0.74, compared to 0.5 for the MISR operational retrieval. These improvements occur primarily when AOD < 0.2 for ANG and AOD < 0.5 for AAOD. Spatial and temporal differences among the aerosol optical properties of MISR V22, GOCART, and the adjusted MISR are traced to (1) GOCART underestimation of AOD and ANG in polluted regions; (2) aerosol mixtures lacking in the MISR Version 22 algorithm climatology; (3) low MISR sensitivity to particle type under some conditions; and (4) parameters and thresholds used in our method.

1 Introduction

Atmospheric aerosols affect global climate directly by absorbing and reflecting solar radiation (Myhre, 2009) and indirectly by altering cloud microphysics and biogeochemical cycles (Mahowald, 2011). Despite several decades of research, the quantitative relationships among aerosols, clouds, and precipitation within the global climate system are still not well understood due to the inadequacy of existing tools and methodologies (Stevens and Feingold, 2009) and available measurements. Aerosol particles originate from a wide variety of natural and anthropogenic sources, and can contain chemically distinct species, such as sulfates, nitrates, organic carbon (OC), black carbon (BC), sea salt, and mineral dust. The concentration and composition of these species are highly variable temporally and spatially. Ground-based observations, such as those provided by the AErosol RObotic NETwork (AERONET), are often used to constrain column-effective aerosol optical properties, but these point measurements have very limited spatial coverage (Holben et al., 1998), and the derivation of particle properties other than the

spectral optical depth or Ångström exponent (ANG) requires many assumptions. During the past decade, researchers have explored the potential of using satellite-retrieved aerosol properties to fill gaps not covered by ground observations. Satellite products have advanced our understanding of aerosol impacts on global climate change (Lohmann and Lesins, 2002), particle type (Kahn and Limbacher, 2012; Liu et al., 2007a), and air quality (Liu et al., 2009b; van Donkelaar et al., 2010).

Uncertainties in satellite aerosol retrievals are usually attributed to cloud contamination, surface reflectance estimation, and the selection of aerosol optical models (Chu et al., 2002). Among these factors, the aerosol models are usually derived from the analysis of ground-based observations, such as AERONET data or aircraft in situ measurements acquired during field campaigns. Omar et al. (2005) found that six aerosol models (representing desert dust, biomass burning, background/rural, polluted continental, marine, and dirty pollution aerosol) characterize the primary aerosol types in almost the entire AERONET data set. With slight modifications, these general aerosol types are used in the operational Cloud–Aerosol Lidar and Infrared Pathfinder Satellite Observation (CALIPSO) lidar aerosol classification algorithm. As the most widely used satellite aerosol data source, NASA's Moderate-Resolution Imaging Spectroradiometer (MODIS) aerosol optical depth (AOD) algorithm assigns a set of global aerosol models in its dark target (DT) algorithm based on spatial and temporal information derived from AERONET (Levy et al., 2013). Many researchers also use local observations to fill the gaps in satellite data needed to create regional aerosol products. For example, Li et al. (2005a) derived seasonal aerosol mixing ratios with single-scattering albedo (SSA) around 0.91–0.94 to accommodate the higher aerosol absorption encountered in Hong Kong. Lee and Kim (2010) achieved better AOD correlations with AERONET than those obtained from the operational MODIS aerosol products when using aerosol models developed by statistically clustering observational data from East Asia. However, AERONET coverage is not dense enough to capture all the subtlety in aerosol-type diversity on continental scales. To date, many studies have demonstrated that atmospheric chemical transport models (CTMs) can help constrain satellite aerosol retrievals under some circumstances. Drury et al. (2008, 2010) first coupled the simulated aerosol properties from a global 3-D chemical transport model (GEOS-Chem) to improve the MODIS DT algorithm. This method was extended by Wang et al. (2010) and Li et al. (2013), who looked specifically at dust and haze pollution in China and demonstrated that customized retrievals performed better than the MODIS standard product in these regions. Although the accuracy of most CTM simulations, like those from GEOS-Chem, depends heavily on the quality of meteorological inputs, atmospheric chemistry schemes, and emission inventories, CTM simulations have the advantage of providing information on aerosol mass con-

centration, composition, and optical properties at regional-to-global scales with complete temporal and spatial coverage. Most importantly for the current study, aerosol type in the model depends primarily on the aerosol source inventories used and is therefore far less sensitive to the ambient AOD downwind than the satellite aerosol-type retrievals.

The MODIS instruments have proven valuable for retrieving AOD around the world, but the standard DT algorithm shows poor performance over bright surfaces and lacks the capability to retrieve additional aerosol optical properties, such as particle type. The analysis presented in this paper focuses on the Multi-angle Imaging SpectroRadiometer (MISR), which was launched into a sun-synchronous polar orbit in December 1999 aboard the NASA Earth Observing System (EOS) Terra satellite. Unlike MODIS, MISR, which has a unique design of nine individual cameras, uses the presence of angular-spatial patterns within a 17.6 km retrieval region to derive an empirical orthogonal function (EOF) representation of region-averaged, surface-leaving light reflection (Martonchik et al., 2009). The EOF algorithm can greatly reduce the impact of surface reflectance uncertainties on aerosol retrievals (Diner et al., 2005). Global validation of MISR-retrieved AOD against AERONET observations showed that the operational (Version 22) MISR AOD product has a retrieval error that falls within a confidence envelope defined by ± 0.05 or $\pm 0.2\tau$, whichever is larger (Kahn et al., 2010). The retrieval algorithm that generates this product defines 74 aerosol optical models (called "mixtures" in MISR terminology), which are combinations of up to three of eight individual aerosol components. Each component is defined by a size distribution, shape, and complex index of refraction. The top-of-atmosphere (TOA) reflectances calculated based on these aerosol mixtures and stored in a look-up table are compared with the observed reflectances. A set of chi-square statistical tests is then applied to determine which aerosol mixtures best fit to the observations (Kahn et al., 1998; Liu et al., 2009a). Using this approach, the MISR aerosol retrieval algorithm provides some particle-type information under favorable retrieval conditions, such as constraints on ANG and SSA, in addition to AOD.

However, the V22 MISR aerosol retrieval approach also has limitations. Although the mixtures included in the MISR algorithm were derived primarily from field measurements, selections among these mixtures are based on a set of chi-square statistical tests that do not employ any prior spatial or temporal aerosol information (e.g., the prior information from AERONET that defines the aerosol optical properties used in the MODIS DT algorithm). If many different mixtures pass the retrieval acceptance criteria, this usually indicates that the aerosol-type information content of the observations is limited (Kahn et al., 2010), and the retrieved type might reflect more on the MISR algorithm aerosol climatology than the true aerosol properties (Liu et al., 2007a, b). Liu et al. (2007a) reported $\sim 20\%$ uncertainty in MISR-retrieved

aerosol microphysical properties when distinguishing light-absorbing and non-light-absorbing aerosols. The sensitivity of the V22 MISR retrieval algorithm to aerosol component information also diminishes when AOD is below 0.15 or 0.2 (Kahn et al., 1997, 2001). Moreover, the V22 MISR algorithm climatology lacks spherical absorbing particles of certain sizes, as well as mixtures containing both spherical, absorbing smoke analogs and non-spherical dust. For these reasons, the V22 MISR algorithm shows poor AOD performance for some biomass burning and urban regions (Kahn et al., 2010; Kahn et al., 2007). ANG also tends to be overestimated in some polluted and smoky regions, as the current set of eight aerosol components in the MISR V22 algorithm lacks medium particles with effective radii between 0.26 and 2.8 μm (Kahn et al., 2010).

Our work aims to add value to MISR-retrieved aerosol optical properties using CTM aerosol simulations as additional constraints on particle types where the MISR radiances lack such sensitivity. We use the Goddard Chemistry Aerosol Radiation and Transport (GOCART) model because it has been evaluated extensively against in situ observations, sun photometer measurements, and satellite observations around the world (Chin et al., 2002b, 2004, 2007, 2009, 2014), and a global-scale model can provide a useful link between satellite and ground observations. GOCART can provide MISR-corresponding parameters, such as AOD, ANG, and absorbing AOD (AAOD), which can also be evaluated using AERONET observations. The rest of the paper is organized such that Sect. 2 describes the data sets involved in this analysis and the methods used for constraining MISR mixtures with CTM simulations. Section 3 validates our method using 4 years of coincident AERONET observations over the contiguous USA. The sources of uncertainties and sensitivity analyses are also discussed in detail in this section. Finally, major findings and potential future improvements to the current analysis are summarized in Sect. 4.

2 Data and method

2.1 MISR aerosol product

The V22 MISR Level 2 aerosol data, with a spatial resolution of 17.6 km, were downloaded from the NASA Langley Research Center Atmospheric Sciences Data Center (http://eosweb.larc.nasa.gov) for the contiguous USA from 2006 through 2009. Total column AOD values used in this analysis are from MISR parameters "RegBestEstimateSpectralOptDepth" and "RegLowestResidSpectralOptDepth" (called "MISR Best Estimate" and "MISR Lowest Resid" hereinafter), which represent the mean AOD of all mixtures that pass the goodness-of-fit tests and the AOD of the mixture with the smallest chi-square, respectively. The corresponding parameters for ANG ("RegBestEstimateAngstromExponent" and "RegLowestResidAngstrom-

Exponent") and SSA ("RegBestEstimateSSA") were also extracted. The ANG reported in the MISR product is calculated from the slope of a linear least-squares fit to the logarithm of the AODs retrieved at MISR's four wavelengths (446, 558, 672, and 866 nm). The AAOD ($\tau^{\text{absorbing}}$) at a given wavelength can be calculated from SSA and AOD as follows:

$$\tau^{\text{absorbing}} = \tau \times (1 - \omega). \tag{1}$$

MISR's 74 mixtures are made of up to three "pure" aerosol components corresponding to spherical non-absorbing aerosol (components 1, 2, 3, and 6, representing optical analogs for sulfate, sea salt, organic aerosol, etc.); spherical, absorbing aerosol (components 8 and 14, representing black or brown carbon particles, etc.); and non-spherical dust analogs (components 19 and 21) (Kahn et al., 2010). A "mixture data" table for the MISR product (as shown in Fig. 1) lists each mixture's properties, such as ANG (reported as "Ångström exponent"), SSA (reported as "mixture spectral single-scattering albedo"), and the fractional contribution of each component to the total mid-visible AOD (reported as "component fractional optical depth in reference band"). MISR also provides information on whether each mixture passed the goodness-of-fit tests (reported as "AerRetrSuccFlagPerMixture"), the number of successful mixtures (reported as "NumSuccAerMixture"), and the green-band (558 nm) AOD for each of the 74 mixtures used in the retrieval (reported as "OptDepthPerMixture"). Therefore, the aerosol optical properties can be calculated based on these mixtures and their related information.

2.2 GOCART aerosol simulations

The NASA GOCART model is driven by assimilated meteorological fields, which are generated in the Goddard Earth Observing System Data Assimilation System (GEOS DAS). Although the GOCART model has been validated around the world (Chin et al., 2009), we also conduct a focused validation study for the same period and geographic region as the MISR retrievals considered in the current study. The GOCART 2-D simulations used in this analysis are at a 3 h temporal resolution and 1° latitude × 1.25° longitude horizontal resolution. Total column AOD (τ) at 550 nm is the sum of five tracer AODs: sulfate, dust, OC, BC, and sea salt:

$$\tau = \tau_{\text{sulfate}} + \tau_{\text{dust}} + \tau_{\text{OC}} + \tau_{\text{BC}} + \tau_{\text{sea-salt}}. \tag{2}$$

GOCART saves 2-D AODs at seven wavelengths (350, 450, 550, 650, 900, 1000, and 1500 nm). ANG is calculated from AODs at 450 and 900 nm using the Ångström equation $\left(\alpha = -\frac{\ln \frac{\tau_{450}}{\tau_{900}}}{\ln \frac{450}{900}} \right)$. The model also provides the AAOD at seven wavelengths for each tracer; thus, the total AAOD at 550 nm ($\tau^{\text{absorbing}}$) can be calculated as

$$\tau^{\text{absorbing}} = \tau_{\text{dust}}^{\text{absorbing}} + \tau_{\text{OC}}^{\text{absorbing}} + \tau_{\text{BC}}^{\text{absorbing}}. \tag{3}$$
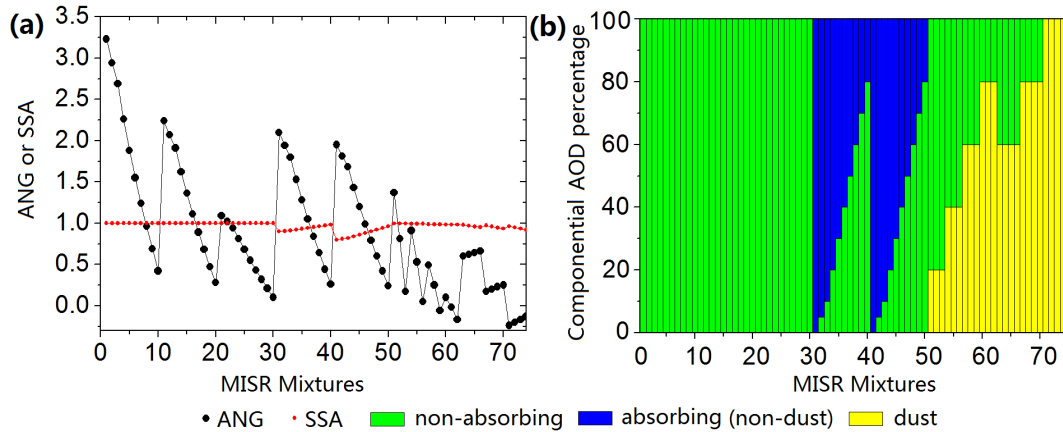
Figure 1. Graphical representation of the 74 aerosol mixtures in the MISR Version 22 standard product. Distributions of **(a)** Ångström exponent and SSA at 558 nm; **(b)** AOD percentages, by component categories, for each mixture.

The factors that affect GOCART AOD the most are the particle mass and the assumed aerosol optical properties. The uncertainties in the simulated aerosol mass are attributed primarily to ground emissions, meteorological fields, and parameterized aerosol removal mechanisms. Because sulfate and sea salt particles are non-absorbing at visible wavelengths, they are not included in Eq. (3).

As shown in Fig. 2, we split the contiguous USA into 690 GOCART grid cells. To compare the satellite retrievals with model simulations, all cloud-free, 17.6 km MISR pixels located in each $1° × 1.25°$ GOCART grid cell were first averaged (called MISR$_{GOCART}$ hereinafter). Then, GOCART simulations at 12:00 LT, which roughly corresponds to the MISR overpass time (∼ 10:30 LT), were sampled for the MISR$_{GOCART}$ swath. Figure 2 also adds the National Land Cover Database (NLCD) 2006 land cover layer, which is partly linked to the ground emission conditions (Wang et al., 2012). Due to the large, systematic differences in land cover, climate, and emissions, we divided the contiguous USA into eastern and western regions along the 100° W longitude line.

2.3 AERONET Level 2 data

Level 2 (quality-assured) spectral AOD data from 32 AERONET sites over the contiguous USA were included in this study (accessed at http://aeronet.gsfc.nasa.gov). As shown in Fig. 2, 14 of these AERONET sites (red circles) are in the eastern USA, many of which are located along the Atlantic coast. There are 18 western AERONET sites, many of which are in crop- or forest-covered regions, according to the NLCD 2006 land cover data. Eighteen of the sites (blue circles) reported absorbing AOD and SSA during the study period. AERONET AOD values at 440 and 870 nm were used to calculate ANG using the Ångström equation above, which was then used to interpolate the AOD to 550 nm to compare with the GOCART and MISR AOD data (MISR values are at 558 nm wavelength). AERONET observations were aver-

aged over a 2 h window around the satellite overpass time (i.e., 10:30 LT). Only high-quality AERONET AAOD retrievals (i.e., AOD at 440 nm > 0.4, and solar zenith angle > 50°; Dubovik et al., 2000, 2002) were used in this study.

2.4 Sub-selecting MISR mixtures with GOCART information

As mentioned above, greater uncertainty is indicated in MISR-retrieved aerosol microphysical properties when many mixtures satisfy the retrieval acceptance criteria (Liu et al., 2007a, b). The post-processing technique proposed in this study aims to narrow the selection of mixtures under these circumstances by introducing GOCART aerosol simulation results. Our approach does not require rebuilding the MISR look-up table or rewriting the EOF code. The additional GO-CART information provides some constraints on aerosol size distribution and composition. We use AAOD rather than SSA (ω), as AAOD has a wider dynamic range than SSA.

In practice, we constrain MISR's aerosol mixture selections in the V22 operational product with information from GOCART model simulation results by calculating the differences of ANG and AAOD between MISR and GOCART:

$$\mathrm{Diff}_{ANG} = |\alpha_{MISR} - \alpha_{GOCART}| \leq \varepsilon_{ANG}, \tag{4}$$

$$\mathrm{Diff}_{AAOD} = |\mathrm{Fraction}_{MISR\_AAOD} \\ - \mathrm{Fraction}_{GOCART\_AAOD}| \leq \varepsilon_{AAOD}, \tag{5}$$

where α is the ANG, and ε_{ANG} and ε_{AAOD} represent the corresponding thresholds for the ANG and AAOD differences at 558 nm, respectively. Fraction$_{MISR\_AAOD}$ is the fractional contribution of AAOD to the total AOD for a specific mixture at 558 nm. The corresponding Fraction$_{GOCART\_AAOD}$ is calculated as $\frac{\tau_{GOCART}^{absorbing}}{\tau_{GOCART}}$. By using fractional AAOD values, Eq. (5) emphasizes the contribution of absorbing aerosol, and it reduces the impact of differences in the absolute AAOD due
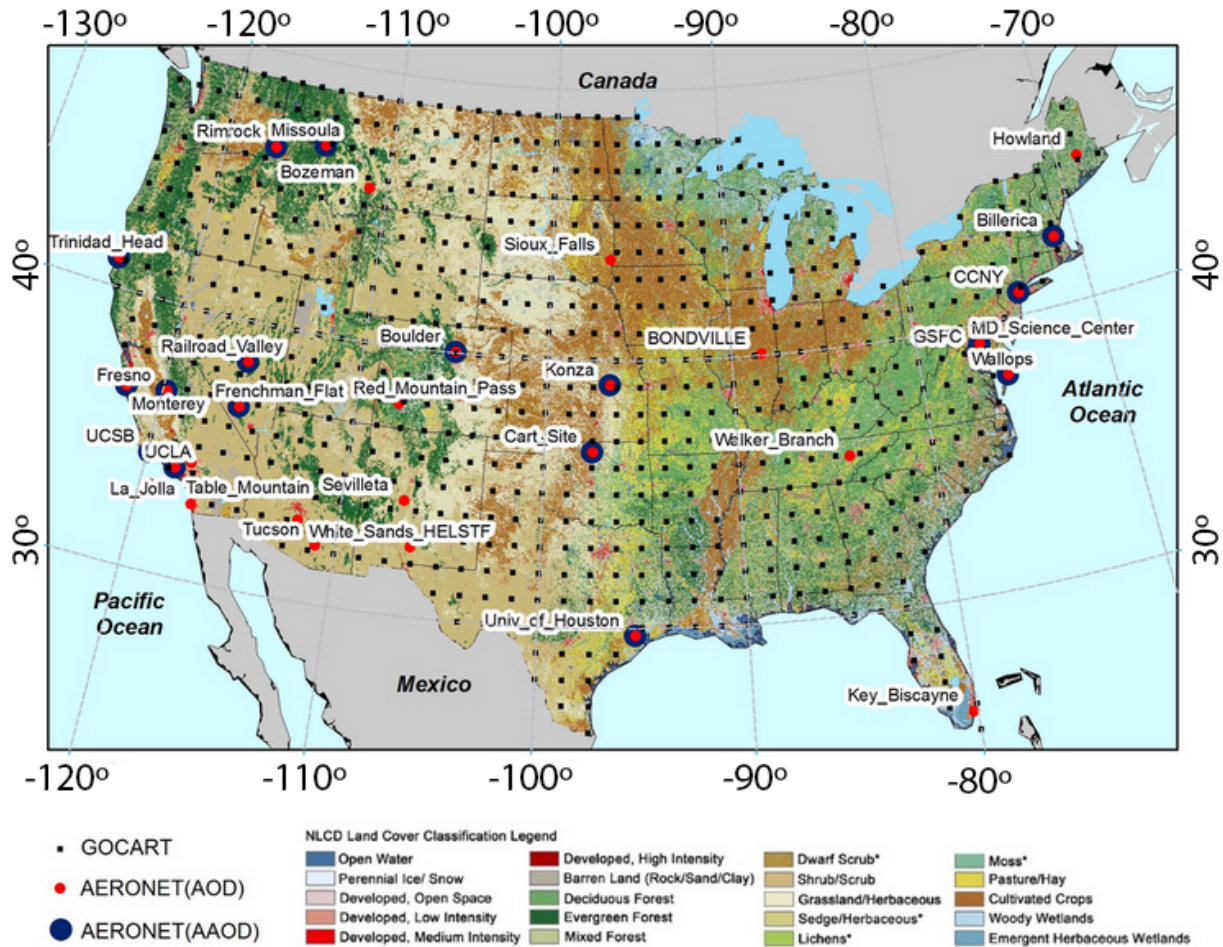
Figure 2. Spatial distribution of GOCART $1° \times 1.25°$ grid points (blue dots), superposed on a map of the contiguous USA. Thirty-two AERONET sites containing AOD Level 2 data from 2006 to 2009 are shown as red dots; those also reporting SSA have a surrounding blue circle. The NLCD 2006 land cover layer, created by the Multi-Resolution Land Characteristics (MRLC) Consortium (http://www.mrlc.gov/nlcd06_data.php), underlies the grid data.

to model–satellite discrepancies, such as resolution differences, satellite retrieval errors, and the impact of emission inventory choices on the model. Because fixed thresholds of ε_{ANG} or ε_{AAOD} often leave no mixtures that meet the acceptance criteria, we adopted dynamic thresholds in Eqs. (4) and (5) to retain a certain percentage of mixtures. Specifically, we first sort the absolute differences calculated by Eqs. (4) and (5) for all the successful mixtures in order from small to large values. We then retain a certain percentage of the successful mixtures based on Eqs. (4) (called ε_{ANG}% hereinafter) and (5) (called ε_{AAOD} % hereinafter). Finally we select the common ones from the two sets of retained mixtures. The minimum (0 %) and maximum (100 %) values represent none and all MISR successful mixtures passing our thresholds, respectively. If no common mixtures are found, we select one mixture with the smallest ε_{ANG} and one with the smallest ε_{AAOD}. We call the aerosol optical properties calculated from the selected MISR-retrieved mixtures "adjusted

MISR" aerosol properties. We adopt this approach primarily to help in situations where the MISR radiances lack aerosol-type information, and many mixtures pass. The errors in our method are mainly due to the uncertainties in the GOCART simulations; limitations in the V22 MISR mixture options; and thresholds of ε_{ANG} % or ε_{AAOD} %, which are discussed in later sections.

3 Results and discussion

3.1 Validation of MISR and GOCART products with AERONET observations

During the period 2006 through 2009, there were 1492 MISR–AERONET matched data records for AOD and ANG over the 32 AERONET sites. Figure 3 and Table 1 show that both MISR Best Estimate and MISR Lowest Resid AOD retrievals are strongly correlated with AERONET data.

Table 1. Validations of MISR, GOCART, and our work's aerosol optical properties by AERONET in different AOD conditions.

	Range		N	Mean_A	Mean	SD	Slope (error)	Intercept (error)	r or γ
AOD	All	MISR1	1492	0.1	0.13	0.056	0.8 (0.015)	0.05 (0.002)	0.79
		MISR2			0.13	0.058	0.8 (0.016)	0.05 (0.002)	0.78
		GOCART			0.09	0.045	0.27 (0.013)	0.06 (0.002)	0.5
		Adj. MISR			**0.13**	**0.057**	**0.79 (0.015)**	**0.05 (0.002)**	**0.79**
ANG	All	MISR1	1492	1.27	1.26	0.42	0.28 (0.02)	0.91 (0.03)	0.29
		MISR2			1.29	0.49	0.24 (0.03)	0.96 (0.04)	0.23
		GOCART			1.17	0.25	0.26 (0.01)	0.84 (0.02)	0.43
		Adj. MISR			**1.21**	**0.26**	**0.29 (0.01)**	**0.84 (0.02)**	**0.45**
	AOD ≤ 0.2	MISR1	1336	1.23	1.24	0.42	0.25 (0.02)	0.93 (0.03)	0.28
		MISR2			1.35	0.49	0.19 (0.03)	1 (0.04)	0.18
		Adj. MISR			**1.18**	**0.26**	**0.27 (0.01)**	**0.86 (0.02)**	**0.42**
	AOD ≥ 0.2	MISR1	156	1.55	1.4	0.39	0.44 (0.08)	0.73 (0.24)	0.4
		MISR2			1.49	0.39	0.57 (0.08)	0.59 (0.13)	0.49
		Adj. MISR			**1.38**	**0.25**	**0.42 (0.05)**	**0.74 (0.08)**	**0.5**
AAOD	All	MISR1	107	0.018	0.009	0.01	0.36 (0.04)		0.5
		MISR2			0.01	0.011	0.39 (0.05)		0.56
		GOCART			0.009	0.006	0.34 (0.03)		0.5
		Adj. MISR			**0.013**	**0.011**	**0.55 (0.05)**		**0.74**
	AOD ≤ 0.5	MISR1	79	0.015	0.007	0.009	0.27 (0.05)		0.47
		MISR2			0.008	0.01	0.29 (0.05)		0.53
		Adj. MISR			**0.011**	**0.009**	**0.51 (0.05)**		**0.73**
	AOD ≥ 0.5	MISR1	28	0.023	0.014	0.012	0.48 (0.08)		0.61
		MISR2			0.015	0.013	0.53 (0.09)		0.65
		Adj. MISR			**0.018**	**0.016**	**0.6 (0.11)**		**0.75**

N is sample size. MISR1, MISR2, and Adj. MISR represent operational "MISR Best Estimate", "MISR Lowest Resid", and adjusted MISR data from this study, respectively. Mean_A is AERONET mean. SD is standard deviation. "r or γ" represents the correlation coefficients for AOD and ANG, and the mean ratio for AAOD. Results from the current study are highlighted in bold font for easy identification. All the regression slopes are statistically significant ($p < 0.0001$).

The agreement between MISR Best Estimate and MISR Lowest Resid was also reported in previous studies (Liu et al., 2004). Our validation effort confirms that MISR-retrieved AOD is fairly robust, even when the retrieved particle properties are not well constrained, due to the multi-angle nature of the data (Kahn et al., 2001, 2010). Compared to the MISR retrievals, GOCART yields a smaller value for the slope and correlation coefficient against AERONET AOD. Many factors may contribute to these results. The model AOD calculation is based on simulated particle mass and assumed aerosol optical parameters (Martin et al., 2003). First, uncertainties in the simulated aerosol mass may be attributed to the emissions inventories used, wet and dry deposition parameterizations, chemical evolution mechanisms, and meteorological fields (e.g., relative humidity). Second, aerosol composition and microphysical and optical properties – such as particle size distributions, refractive indices and/or hygroscopic growth factors used by the model – are assumed independently and may be incorrect. For example, GOCART does not include nitrate aerosol and does not consider particle in-

ternal mixing. Third, the GOCART simulations at $1° \times 1.25°$ spatial resolution usually do not represent the high AOD near the source within the model grid cell, resulting in lower mean AOD values than AERONET point observations near sources. Nevertheless, the GOCART model reproduces the correct seasonal variability at most sites, especially in places where biomass burning or dust aerosol dominates (Chin et al., 2002a). Table 1 indicates that both the mean value of GOCART AOD over the contiguous USA (0.09) and the standard deviation (SD: 0.045) are comparable with those of AERONET (Mean_A:0.1) and MISR (SD: ~ 0.056).

Linear regression of the MISR Best Estimate ANG against the AERONET observations, for all data regardless of AOD, yields a low correlation and a flat slope (Fig. 3.2a and Table 1). Although the values of ANG among the 74 MISR mixtures have a wide range (from 3.8 to -0.2, as shown in Fig. 1), if many different mixtures meet the MISR algorithm acceptance criteria, ANG calculated from the average of AOD values obtained in each MISR spectral channel tends toward the mean value of unity (Kahn et al., 2009). More-
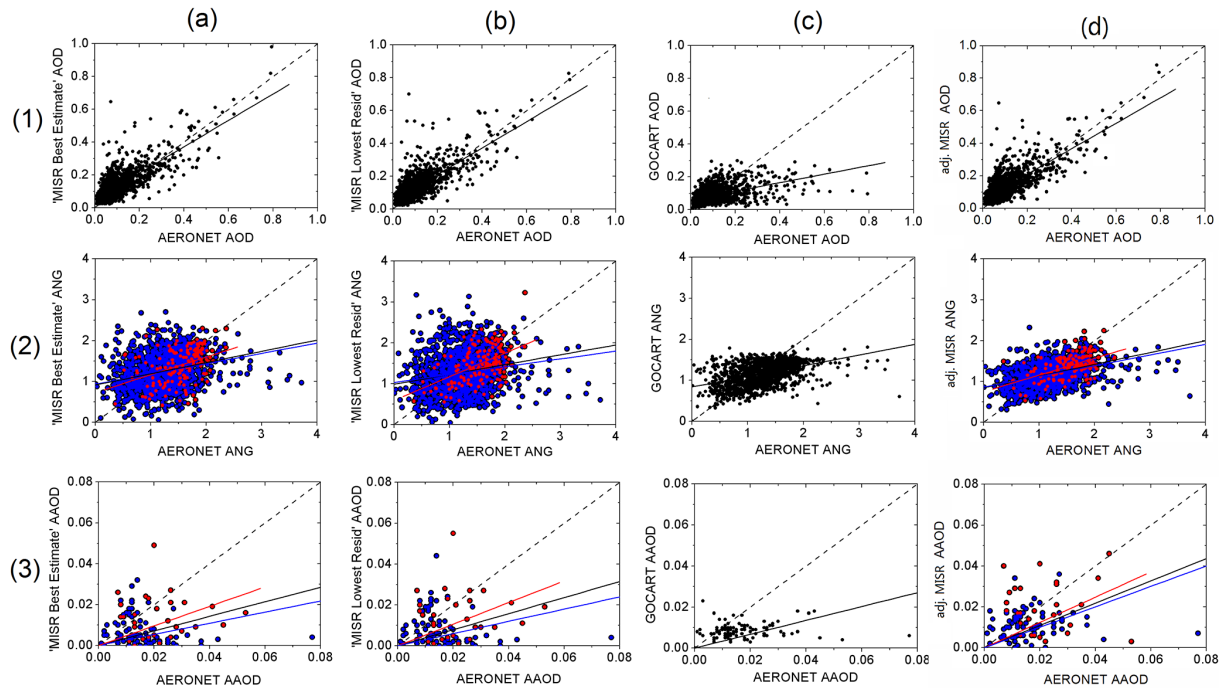
Figure 3. Validation of "MISR Best Estimate" **(a)**, "MISR Lowest Resid" **(b)**, GOCART **(c)**, and AOD from this study **(d)**; AOD along row 1, ANG along row 2, and AAOD along row 3, by comparison with AERONET observations. The black (for rows 2 and 3, over-plotted with blue and red points), blue, and red points represent all AOD, AOD ≤ 0.2, and AOD > 0.2 conditions, respectively. For AAOD, blue and red points are divided at AOD = 0.5 rather than 0.2. The black, blue, and red lines represent the corresponding regression lines. The dashed line is the $y = x$ line. AERONET AAOD is only retrieved when the AOD at 440 nm is greater than 0.4 and the solar zenith angle is larger than 50. Only 107 matched MISR–AERONET AAOD data records are found in our study region.

over, when mid-visible AODs are below about 0.2, which occurs commonly over the USA (1336 records shown in Table 1), the MISR radiances tend to have insufficient information to constrain particle properties (Kahn et al., 2009). This is illustrated by the blue and red points in Fig. 3.2a, which are for AOD ≤ 0.2 and AOD > 0.2, respectively. For the blue points, MISR shows poor ANG retrievals (r: 0.28; SD: 0.49) for the entire data set. However, the correlation coefficient for the red points increases to 0.40, and the SD reduces to 0.39. Similarly, Fig. 3.2b shows the relationships between MISR Lowest Resid and AERONET ANG in black, and MISR Lowest Resid vs. AERONET ANG but separated by AOD = 0.2 in blue and red. Again, the correlation coefficient improves significantly from 0.23 for the entire data set and 0.18 for AOD ≤ 0.2 to 0.49 for AOD > 0.2, and the SD reduces to 0.39.

Although its mean value is lower than MISR, the correlation between GOCART-simulated ANG and AERONET is better than MISR when all data are included, mainly because low AOD does not reduce the aerosol-type information in the model. The lower ANG in GOCART is mainly due to having too weak a spectral dependence of sulfate aerosol extinction resulting from too large a standard deviation for the sulfate particle size distribution, based on the Optical Properties of Aerosols and Clouds (OPAC) database (Hess et al.,

1998), used in calculating the optical properties (Chin et al., 2009). As a result, constraining the MISR results with GOCART in some cases makes the comparison with AERONET poorer than the unconstrained MISR product (Table 1). This demonstrates the dependence of our approach on the quality of the model (but see Sects. 3.3, 3.4, and Table 2 for further discussion). Despite the limitations, the GOCART model is validated against many observations, and it captures the overall spatial and temporal features of aerosol type. Therefore, ANG and AAOD constraints from the model become useful for sub-selecting MISR aerosol type in situations where the retrieval is ambiguous, e.g., when total AOD is less than 0.2, a regular occurrence over the USA (Reid et al., 1999; Russell et al., 2010).

Given that both the AOD and solar zenith angle conditions must be met for such retrievals to be of high quality, there are far fewer AERONET sky-scan AAOD results compared with direct-sun AOD measurements, and many more assumptions are required to derive aerosol absorption. In our analysis, we found only 107 matched MISR–AERONET AAOD data records, compared with 1492 AOD matches, making our results less statistically robust. MISR Best Estimate AAOD at 558 nm, with a mean value of 0.009, is much lower than the AERONET AAOD (0.018), and the SD is as high as 0.01. We calculated the ratio of mean retrieved AAOD to mean

AERONET AAOD (γ : 0.5) and the regression slope (0.36), i.e., with zero intercept, to show its underestimation, and no meaningful correlation coefficient is derived due to the poor agreement. MISR Lowest Resid AAOD shows similar underestimation with a γ of 0.56, a slope of 0.39, and a SD of 0.011. This is expected because spherical absorbing aerosol optical analogs are lacking in the V22 MISR aerosol climatology (Kahn et al., 2010), so SSA generally tends to be too high in places where absorbing aerosol occurs, skewing MISR AAOD too low. Another contributing factor is that the aerosol loading in the contiguous USA is too low to provide more AAOD or SSA information in the MISR radiances. We analyzed the AAOD comparison for AOD > 0.5 (red points in Fig. 3.3a and b) and AOD ≤ 0.5 (blue points). Both MISR Best Estimate and MISR Lowest Resid AAOD ratios (γ) are greater than the overall mean ratio when AOD > 0.5, and are lower when AOD ≤ 0.5. The GOCART model also underestimates the AAOD with a γ of 0.43, but it provides a more linear trend when compared with AERONET (Fig. 3.3c). A previous study also found similar underestimation for GOCART AAOD simulations over the USA (Chin et al., 2009). The adjusted MISR AAOD takes advantage of GOCART simulations' better trend and achieves greater γ values at both AOD value ranges (Fig. 3.3d and Table 1). Note that the adjusted AAOD value can come out higher than both the MISR and GOCART values because the AAOD threshold is based on the ratio of AAOD over AOD rather than the AAOD values themselves.

3.2 Sensitivity analysis and validation of our algorithm

Our validation suggests that the MISR Best Estimate and MISR Lowest Resid parameters could be used essentially interchangeably for AOD, and both parameters show generally poor performance for ANG and AAOD in the study region. We chose MISR Best Estimate, which contains more mixtures, to represent the MISR-retrieved aerosol parameters. The goal of the sensitivity analysis in this section is to select the optimum ε_{ANG} % and ε_{AAOD} % to achieve better agreement between adjusted MISR AOD, ANG, and AAOD results and those of AERONET. We used the correlation coefficients of AOD (r_{AOD}) and ANG (r_{ANG}) between adjusted MISR and AERONET and the ratio of mean adjusted MISR AAOD to mean AERONET AAOD (γ_{AAOD}) to measure the performance of our method. Figure 4 shows the distributions of r_{AOD}, r_{ANG}, and γ_{AAOD}, with ε_{ANG} % and ε_{AAOD} % varying from 0 to 100 %. When both ε_{ANG} and ε_{AAOD} are 100 %, our r_{AOD}, r_{ANG}, and γ_{AAOD} are equal to the corresponding original MISR correlation coefficients and ratios in Table 1.

1. AOD: when ε_{ANG} % or ε_{AAOD} % is lower than 30 %, our r_{AOD} increases with the number of successful mixtures. When both ε_{ANG} % and ε_{AAOD} % are larger than 30 % (inside the red region of Fig. 4a), r_{AOD} is stable at a relatively high value (> 0.75), almost equal to the
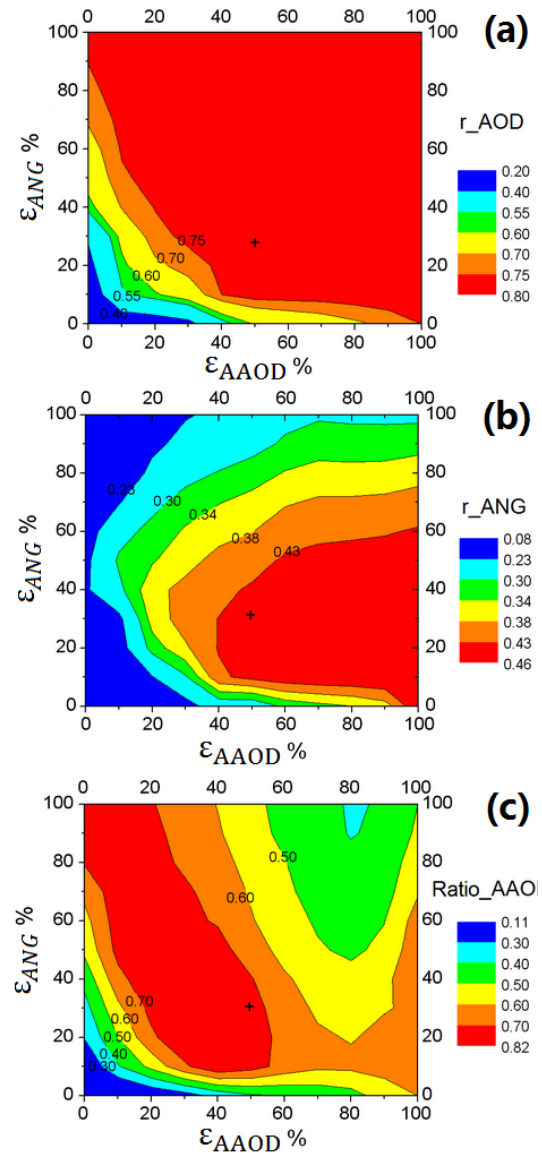
Figure 4. Sensitivity analysis for correlations between adjusted MISR **(a)** AOD, **(b)** ANG, **(c)** AAOD and AERONET by thresholds of ANG and AAOD. The axes specify the percent of mixtures passing the MISR retrieval acceptance criteria coming closest to the GOCART model value that is retained by our method (Eqs. 4 and 5), so a smaller number means the model is used to provide a tighter constraint. The resulting agreement is then assessed based on MISR–AERONET coincident observations. The color from blue to red represents the correlation coefficients (for AOD of Fig. 4.a and ANG of Fig. 4.b) or the mean ratio (for AAOD of Fig. 4.c) from low to high; so for each panel, colors toward "red" indicate better MISR–AERONET agreement when the GOCART–MISR agreement criteria specified by the axes are applied.

original $r_{MISR-AOD}$ (0.79) in Fig. 3a. Our findings here indicate that MISR AOD is at least as good as – and is generally better than – the corresponding GOCART values for mid-visible AOD below about 0.15 or 0.2. In

Table 2. The correlation coefficients (for AOD and ANG) and mean ratio (for AAOD) between MISR, our result (in the specific thresholds), and AERONET.

		ε_{ANG} %	ε_{AAOD} %	$r\_$AOD	$r\_$ANG	$\gamma\_$AAOD
East	MISR			0.86	0.2	0.5
	Adj. MISR	**20 %**	**50 %**	**0.86**	**0.41**	**0.68**
West	MISR			0.68	0.26	0.48
	Adj. MISR	**30 %**	**50 %**	**0.7**	**0.42**	**0.99**
Spring	MISR			0.59	0.27	0.34
	Adj. MISR	**20 %**	**40 %**	**0.58**	**0.5**	**0.41**
Summer	MISR			0.73	0.43	0.52
	Adj. MISR	**30 %**	**100 %**	**0.74**	**0.48**	**0.93**
Fall	MISR			0.86	0.18	0.55
	Adj. MISR	**40 %**	**40 %**	**0.87**	**0.24**	**0.98**
Winter	MISR			0.76	0.27	0.25
	Adj. MISR	**40 %**	**60 %**	**0.77**	**0.3**	**0.47**

$T\_$ANG and $T\_$AAOD are the thresholds of ANG and AAOD, respectively. Results from the current study are highlighted in bold font for easy identification.

general, MISR AOD retrievals contain unique information that the transport model is unlikely able to improve upon, except to the extent that aerosol type affects the result, which occurs preferentially at higher AOD (Kahn et al., 2001, 2010).

2. ANG: our r_{ANG} is negatively correlated with ε_{ANG} %, as might be expected (requiring tighter MISR–GOCART ANG agreement produces better correlation with AERONET), but is generally positively correlated with ε_{AAOD} %. When ε_{AAOD} % is low, r_{ANG} usually increases with the ε_{AAOD} % value, indicating better ANG results when very tight agreement with transport model absorption is not imposed. This is probably related to the MISR V22 climatology containing only a single size of spherical absorbing particles (Kahn et al., 2010). When ε_{AAOD} % is larger than 40 %, r_{ANG} depends only on ε_{ANG} %, reflecting greater MISR sensitivity to particle size than absorption (Kahn et al., 1998). Our analysis indicates that setting a relatively stringent (low) GOCART ANG threshold can significantly improve the correlation between MISR ANG and AERONET. As shown in the red region of Fig. 4b, r_{ANG} approaches 0.43, which is much higher than $r_{MISR-ANG}$ unconstrained by the model (0.29 in Fig. 3.2a).

3. AAOD: the relationship between γ_{AAOD} and the values of ε_{AAOD} % and ε_{ANG} % is complex (Fig. 4c). When ε_{AAOD} % is between about 20 and 80 %, γ_{AAOD} is negatively correlated with ε_{AAOD} %. In this regime, a tighter GOCART constraint on the MISR mixtures improves MISR–AERONET AAOD agreement. γ_{AAOD} also improves somewhat with a tighter ε_{ANG} % constraint, at least when ε_{AAOD} % $> \sim 50$ %. However, when ε_{AAOD} %

$< \sim 40$ %, γ_{AAOD} is relatively independent of ε_{ANG} %. That is, given the MISR V22 algorithm aerosol mixture climatology, constraining the retrieved particle size with the model contributes to improving γ_{AAOD} when the model-based AAOD constraint on the retrieval is loose, but less so when it is tight. As shown in the red region of Fig. 4c, when ε_{AAOD} % is lower than roughly 60 % and ε_{ANG} % is higher than 20 %, γ_{AAOD} could be in the range of ~ 0.7–0.82, which is much higher than the original $\gamma_{MISR-AAOD}$ (0.5) in Fig. 3.3a.

A set of appropriate thresholds should improve r_{ANG} and at least not diminish r_{AOD}, while keeping γ_{AAOD} as close to 1.0 as possible. Note that these thresholds are optimized only for a given data set. For example, by checking the overlapping red regions among Figs. 4a, b, and c, we set ε_{ANG} % and ε_{AAOD} % to 30 and 50 %, respectively, for the entire data set (the black crosses in each panel of Fig. 4). Plots similar to Fig. 4, but stratified by season and region, are given in the Supplement (Fig. S1).

3.3 Validation of adjusted MISR aerosol optical properties

Given the different influences of GOCART aerosol simulations on MISR aerosol retrievals, we divided our data into two groups (ANG is grouped by AOD ≤ 0.2 and AOD > 0.2; AAOD is grouped by AOD ≤ 0.5 and AOD > 0.5). The corresponding thresholds and results are presented in Table 2. The agreement between adjusted MISR AOD and AERONET is similar to that of the MISR operational product (Fig. 3 and Table 1). As expected, the GOCART-based aerosol-type constraints have little effect on MISR AOD over the contiguous USA.
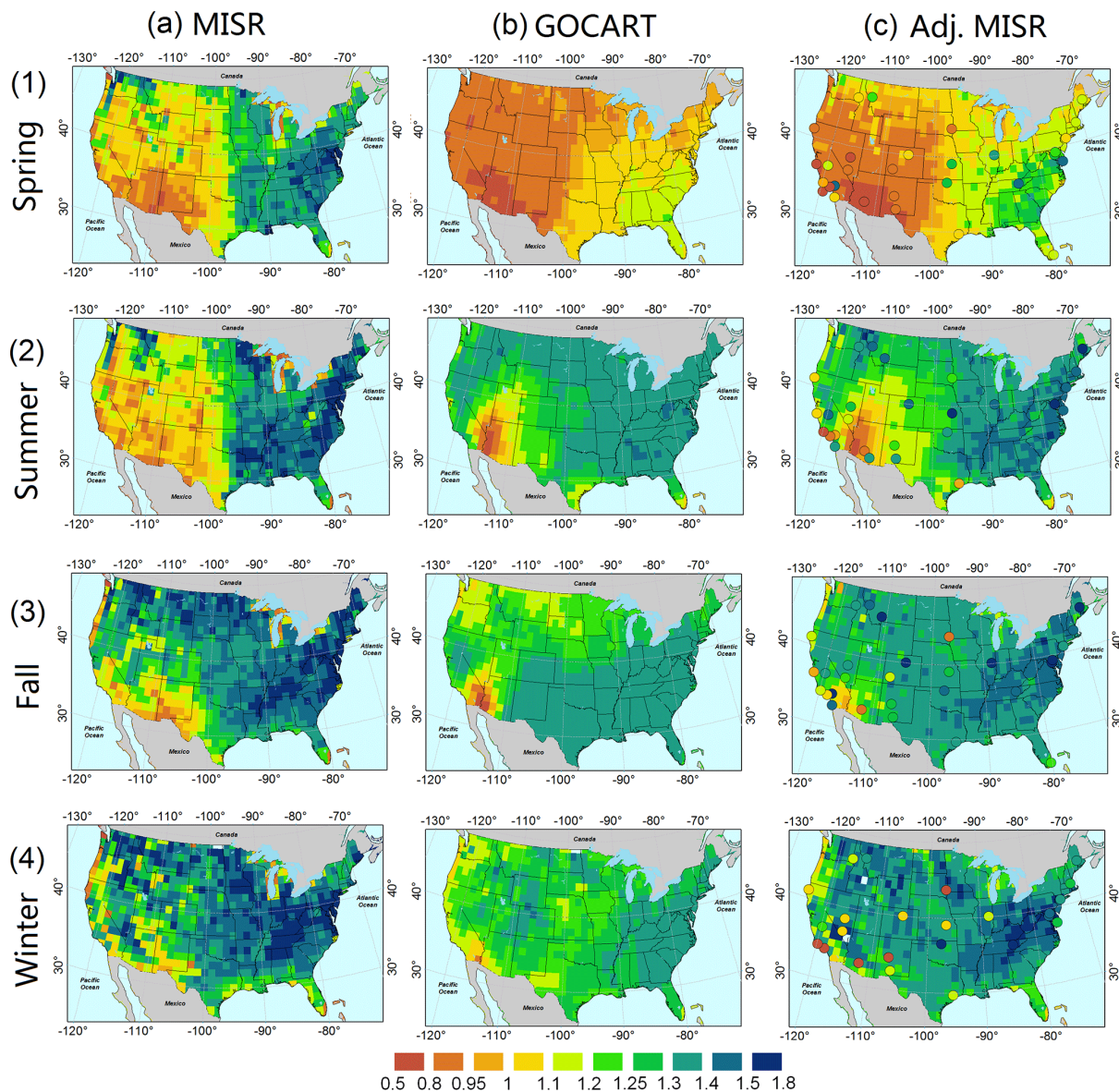
Figure 5. Distributions of seasonally averaged ANG from MISR retrievals **(a)**, GOCART simulations **(b)**, this study **(c)**, and AERONET measurements (superposed as circles in column c) for the years 2006 to 2009, in spring (row 1), summer (row 2), fall (row 3), and winter (row 4). AERONET and GOCART data are temporally and spatially matched to MISR cloud-free conditions.

Although the mean adjusted MISR ANG is slightly worse than the operational MISR data due to the low bias in GOCART, the SD, slope, and correlation coefficient of the adjusted MISR retrievals are all in better agreement with AERONET (Table 1 and Fig. 3d). Table 2 indicates that the greatest improvement is found in spring, probably because GOCART simulates springtime dust emissions well.

For AAOD, our method generates more accurate mean AAOD and ratio than operational MISR data (Table 1). Especially where MISR information content is lacking (AOD ≤ 0.5), the adjusted MISR AAOD is closer to AERONET than the operational data, and the improvements

are more significant than those when AOD > 0.5. Results in certain seasons or regions are stronger than for the data set taken as a whole. For example, Table 2 shows that the ratios in the west and in the fall are close to 1, almost a factor of 2 higher than those of the operational MISR product. However, these results should be treated with caution given the very small sample size.

3.4 Spatial-temporal patterns of MISR, GOCART, and our aerosol optical properties

We compared the seasonal distribution of ANG to AAOD (Figs. 5 to 6) of MISR, GOCART, and adjusted MISR data
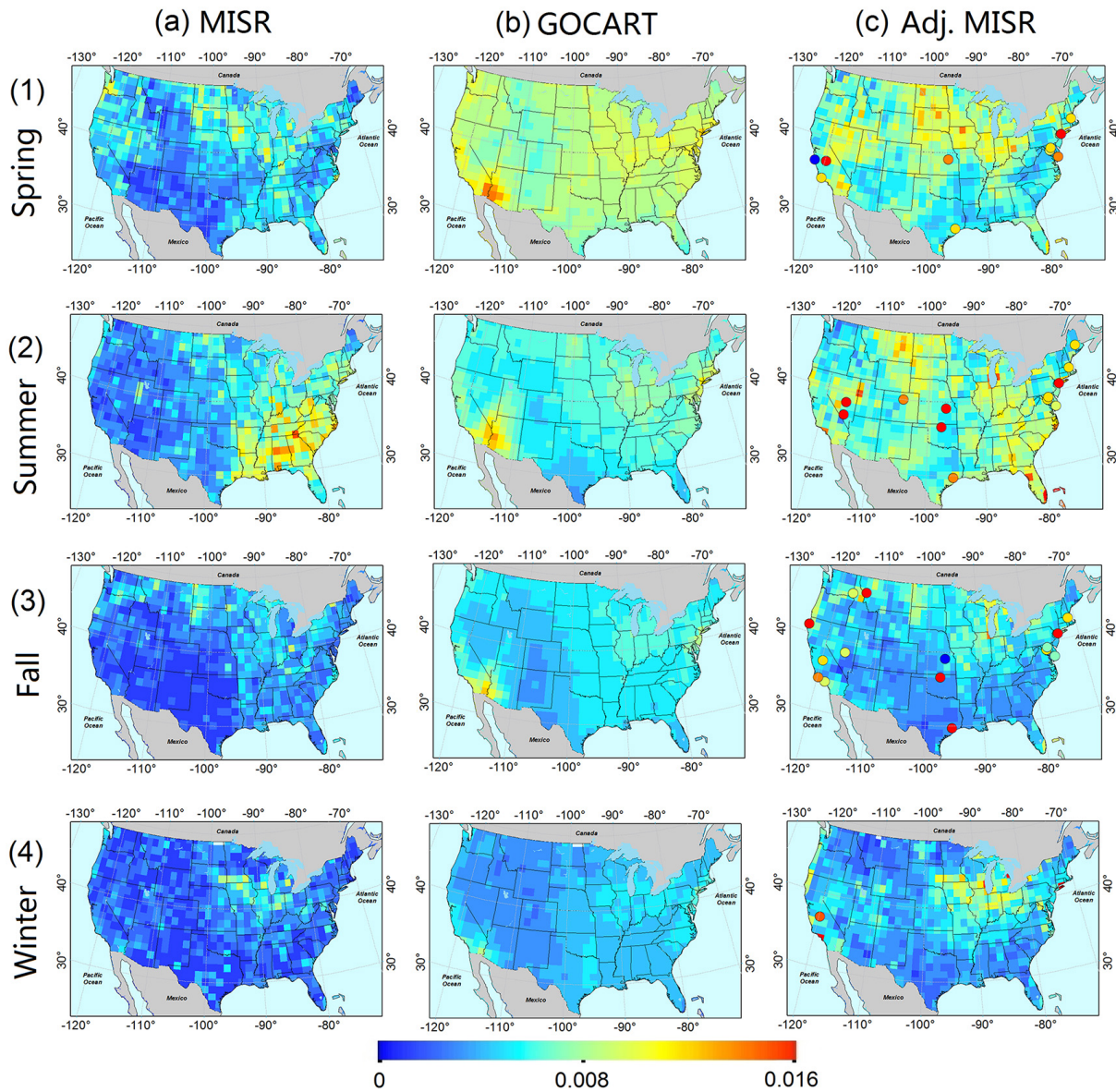
Figure 6. Same as Fig. 5, but for AAOD distributions. Note the color bar is from 0 to 0.016.

over the contiguous USA. We also present the mean value of the entire data set, as well as the data stratified by season and location, in Table 3. As the adjusted AODs are very similar to the original MISR values, the associated maps are given in the Supplement (Fig. S2). In addition to calculating a direct mean value, we also characterized the AOD, ANG, and AAOD number distributions according the value bins (Fig. S3). Our statistics are consistent with a previous multi-year, multi-site AOD validation study (O'Neill et al., 2000). GOCART, MISR, and adjusted MISR AOD data all follow lognormal distributions for the entire data set and regional and seasonal subsets. ANG appears more Gaussian, and AAOD is too poorly sampled in the available data to

draw a conclusion. The operational MISR and adjusted results are very similar, and both are higher than GOCART.

1. ANG: Fig. 5 and Table 3 show that the spatial-temporal patterns, and the mean value of the adjusted MISR ANG falls between the operational MISR and GOCART values. Geographically, all three data sets show ANG values in the east are significantly higher than those in the west. All three data sets indicate the minimum ANG values are found in spring. The low values found in the west and spring can probably be attributed to dust transport. Yu et al. (2012) found approximately 56 of the 140 Tg of fine dust exported from Asia in the spring of 2005 reached the west coast of North America. The contribution of Asian dust becomes weaker in the sum-

Table 3. Mean values of MISR, GOCART, and our work's aerosol optical properties over the contiguous USA.

		All	East	West	Spring	Summer	Fall	Winter
AOD	MISR	0.14	0.16	0.13	0.17	0.18	0.1	0.083
	GOCART	0.092	0.11	0.079	0.12	0.1	0.075	0.058
	Adj. MISR	**0.14**	**0.15**	**0.13**	**0.17**	**0.18**	**0.097**	**0.082**
ANG	MISR	1.24	1.34	1.16	1.15	1.19	1.32	1.34
	GOCART	1.19	1.24	1.14	0.94	1.28	1.27	1.26
	Adj. MISR	**1.22**	**1.28**	**1.15**	**1**	**1.26**	**1.32**	**1.31**
AAOD	MISR	0.0035	0.0043	0.0023	0.0042	0.0045	0.0027	0.0021
	GOCART	0.0059	0.0061	0.0057	0.0081	0.006	0.0048	0.0039
	Adj. MISR	**0.0059**	**0.006**	**0.0058**	**0.007**	**0.0071**	**0.0044**	**0.0042**

mer and fall, and decreases to 30–50 % of the springtime maximum over the eastern USA (Fairlie et al., 2007), although the western USA also has local dust sources. MISR ANG yields large uncertainties when dust particles are abundant, due to the limited, non-spherical dust optical analogs in the V22 climatology. For example, Kalashnikova et al. (2005) found that a lack of very absorbing, plate-like dust particles in the MISR retrieval algorithm climatology can lead to AOD underestimation and might thus introduce ANG biases. In the MISR research algorithm, arbitrarily large numbers of mixtures can be included, each of which can contain up to four individual aerosol components (Kahn et al., 2001). Our findings support the dust analysis and research algorithm conclusions that MISR operational retrievals would benefit from having more dust particle types. Compared to MISR and AERONET data, GOCART ANG values in the east, especially for some northeastern sites (e.g., GSFC), are significantly lower, which is consistent with a previous study (Chin et al., 2009). Overall, the spatial-temporal distribution of the adjusted MISR ANG is more similar to the GOCART distribution than to the operational MISR in the west in spring and summer, but it is more similar to the operational MISR distribution than GOCART in the east in fall and winter. Unlike the lognormal distribution of AOD, our statistics indicate that MISR, GOCART, and the adjusted MSIR ANG data follow approximately normal distributions (Fig. S3).

2. AAOD: Fig. 6 and Table 3 show large AAOD distribution differences among the three data sets. The mean MISR AAOD in the contiguous USA during 2006 to 2009 is much lower than the GOCART and the adjusted MISR AAOD. When we limited our data to those with column MISR AOD values greater than or equal to 0.2, which accounted for about 19 % of the raw data, the mean MISR AAOD increases to 0.0095. As concluded in Sect. 3.1 and in earlier work, it indicates that more AAOD information can be inferred

from the MISR radiances when AOD is high. GO-CART shows smooth regional change in the contiguous USA (mean AAOD around 0.006 for both the east and the west), except high AAOD values in the southwest and northeast, and the values in spring and summer are higher than those during fall and winter. Geographically, the adjusted MISR AAOD distribution shows that the high-absorbing-aerosol regions (e.g., the north and the southeast) are similar to those in the operational MISR product, but the values are closer to those given by AERONET than the operational MISR. Figure 6 indicates that there is a positive relationship between our high AAOD and the NLCD forest and shrubland cover type (Fig. 2), where wildfires or prescribed burns can release more absorbing particles, such as BC and OC (Zhang and Kondragunta, 2008). The anthropogenic and wildfire emissions from western North America are mostly transported north and east, eventually merging with eastern US pollution outflow to the Atlantic (Li et al., 2005b). The presence of elevated aerosol layers from biomass burning outflow across the Gulf of Mexico also has a large impact on the southeast (Wang et al., 2009). Seasonally, the relatively high values in the adjusted MISR AAOD may be caused by dust transport in spring and fire emissions in summer (Ichoku et al., 2008). As mentioned in Sect. 2.4, our AAOD depends not only on the MISR AOD values but also on the fraction of GOCART AAOD and the successful MISR-retrieved mixture distributions. Therefore, making quantitative improvements to the satellite component aerosol retrieval is difficult. First, there are large uncertainties in GOCART data quality and MISR's ability to distinguish light-absorbing and nonabsorbing aerosols (Kahn et al., 2001; Liu et al., 2007a). If fewer absorbing mixtures pass the MISR EOF algorithm and/or an inappropriate GOCART AAOD fraction is used in our method, it would likely result in lower absorbing aerosol levels. Second, the SSA values of predefined mixtures in the V22 MISR climatology overall are too high for the contiguous USA, making the AAOD

too low. To bridge the gaps, new aerosol optical models need to be added to the standard algorithm climatology (Kahn et al., 2010). Our statistics indicate that the AAOD distribution is different from those of AOD (the lognormal distribution) and ANG (the normal distribution). AAOD data appear to follow an approximate exponential distribution, but sampling is too poor to draw strong conclusions, and most values are less than 0.01.

4 Conclusions

We have developed a new method to refine the aerosol optical properties derived in the operational MISR aerosol product over land, with the help of GOCART simulations. We applied this method to the contiguous USA from 2006 to 2009. In this study, we first processed a set of successful MISR mixtures, which contain AOD, ANG, SSA, and aerosol component information. We then used the corresponding GOCART aerosol optical properties to select subsets of those mixtures. Sensitivity analysis shows that setting the ANG and AAOD thresholds at almost 30 and 50 %, respectively, can achieve better agreement between the ANG and AAOD results and those of AERONET for the entire USA than with the operational MISR data. Finally, new aerosol optical properties were calculated from the adjusted mixtures.

We validated the MISR products and GOCART simulations of AOD, ANG, and AAOD using coincident AERONET measurements and estimated the seasonal distributions of these quantities over the contiguous USA from 2006 to 2009. For AOD, GOCART constraints did not provide any statistically significant improvement to the operational MISR AOD values, compared to AERONET. Since GOCART can simulate ANG based on assumed size distributions, which is in some respects closer to AERONET values than retrieved by the V22 MISR algorithm in the study region, using a stringent ANG threshold (30 %) significantly improves the correlation between the adjusted MISR ANG values and AERONET, though the mean ANG value was slightly worsened due to poor assumed particle size distribution in the model. The best agreement is found in spring, probably because GOCART provides good dust simulations. The spatial and temporal distribution of the adjusted ANG tends to be more similar to the GOCART or MISR distribution when either performs well. All three data sets demonstrate the west and the spring have lower ANG values, likely due to the impact of dust. For AAOD, model constraints help bring the underestimated MISR AAOD closer to AERONET. For example, setting an AAOD threshold of 50 % increases the ratio of adjusted MISR AAOD over AERONET to 0.74.

Some of the limitations of this analysis can be addressed by introducing more aerosol components and mixtures into the MISR retrieval algorithm (Kahn et al., 2010). This process will also require building new aerosol look-up tables and rerunning the EOF algorithm. Second, other CTMs could

also be used to constrain MISR mixtures, especially when the information is lacking in the MISR radiances themselves, e.g., at low AOD. More sensitivity analyses should be conducted based on other aerosol parameters and assessment criteria. Finally, similar studies could be carried out in developing countries and other regions that have heavy anthropogenic (or absorbing) aerosols, where aerosol type is not well retrieved by MISR alone.

References

Chin, M., Ginoux, P., Kinne, S., Torres, O., Holben, B. N., Duncan, B. N., Martin, R. V., Logan, J. A., Higurashi, A., and Nakajima, T.: Tropospheric aerosol optical thickness from the GOCART model and comparisons with satellite and Sun photometer measurements, J. Atmos. Sci., 59, 461–483, 2002a.

Chin, M., Ginoux, P., Kinne, S., Torres, O., Holben, B. N., Duncan, B. N., Martin, R. V., Logan, J. A., Higurashi, A., and Nakajima, T.: Tropospheric Aerosol Optical Thickness from the GOCART Model and Comparisons with Satellite and Sun Photometer Measurements, J. Atmos. Sci., 59, 461–483, 2002b.

Chin, M., Chu, A., Levy, R., Remer, L., Kaufman, Y., Holben, B., Eck, T., Ginoux, P., and Gao, Q. X.: Aerosol distribution in the Northern Hemisphere during ACE-Asia: Results from global model, satellite observations, and Sun photometer measurements, J. Geophys. Res.-Atmos., 109, D23S90, doi:10.1029/2004JD004829, 2004.

Chin, Mian, Diehl, T., Ginoux, P., and Malm, W.: Intercontinental transport of pollution and dust aerosols: implications for regional

air quality, Atmos. Chem. Phys., 7, 5501–5517, doi:10.5194/acp-7-5501-2007, 2007.

Chin, M., Diehl, T., Dubovik, O., Eck, T. F., Holben, B. N., Sinyuk, A., and Streets, D. G.: Light absorption by pollution, dust, and biomass burning aerosols: a global model study and evaluation with AERONET measurements, Ann. Geophys., 27, 3439–3464, doi:10.5194/angeo-27-3439-2009, 2009.

Chin, M., Diehl, T., Tan, Q., Prospero, J. M., Kahn, R. A., Remer, L. A., Yu, H., Sayer, A. M., Bian, H., Geogdzhayev, I. V., Holben, B. N., Howell, S. G., Huebert, B. J., Hsu, N. C., Kim, D., Kucsera, T. L., Levy, R. C., Mishchenko, M. I., Pan, X., Quinn, P. K., Schuster, G. L., Streets, D. G., Strode, S. A., Torres, O., and Zhao, X.-P.: Multi-decadal aerosol variations from 1980 to 2009: a perspective from observations and a global model, Atmos. Chem. Phys., 14, 3657–3690, doi:10.5194/acp-14-3657-2014, 2014.

Chu, D. A., Kaufman, Y. J., Ichoku, C., Remer, L. A., Tanre, D., and Holben, B. N.: Validation of MODIS aerosol optical depth retrieval over land, Geophys. Res. Lett., 29, 1617, doi:10.1029/2001GL013205, 2002.

Diner, D. J., Martonchik, J. V., Kahn, R. A., Pinty, B., Gobron, N., Nelson, D. L., and Holben, B. N.: Using angular and spectral shape similarity constraints to improve MISR aerosol and surface retrievals over land, Remote Sens. Environ., 94, 155–171, 2005.

Drury, E., Jacob, D. J., Wang, J., Spurr, R. J. D., and Chance, K.: Improved algorithm for MODIS satellite retrievals of aerosol optical depths over western North America, J. Geophys. Res.-Atmos., 113, D16204, doi:10.1029/2007JD009573, 2008.

Drury, E., Jacob, D. J., Spurr, R. J. D., Wang, J., Shinozuka, Y., Anderson, B. E., Clarke, A. D., Dibb, J., McNaughton, C., and Weber, R.: Synthesis of satellite (MODIS), aircraft (ICARTT), and surface (IMPROVE, EPA-AQS, AERONET) aerosol observations over eastern North America to improve MODIS aerosol retrievals and constrain surface aerosol concentrations and sources, J. Geophys. Res.-Atmos., 115, D14204, doi:10.1029/2009JD012629, 2010.

Dubovik, O., Smirnov, A., Holben, B. N., King, M. D., Kaufman, Y. J., Eck, T. F., and Slutsker, I.: Accuracy assessments of aerosol optical properties retrieved from Aerosol Robotic Network (AERONET) Sun and sky radiance measurements, J. Geophys. Res.-Atmos., 105, 9791–9806, 2000.

Dubovik, O., Holben, B., Eck, T. F., Smirnov, A., Kaufman, Y. J., King, M. D., Tanre, D., and Slutsker, I.: Variability of absorption and optical properties of key aerosol types observed in worldwide locations, J. Atmos. Sci., 59, 590–608, 2002.

Fairlie, T. D., Jacob, D. J., and Park, R. J.: The impact of transpacific transport of mineral dust in the United States, Atmos. Environ., 41, 1251–1266, 2007. Hess, M., Koepke, P., and Schult, I.: Optical properties of aerosols and clouds: The software package OPAC, Bull. Amer. Meteorol. Soc., 79, 831–844, 1998

Holben, B. N., Eck, T. F., Slutsker, I., Tanre, D., Buis, J. P., Setzer, A., Vermote, E., Reagan, J. A., Kaufman, Y. J., Nakajima, T., Lavenu, F., Jankowiak, I., and Smirnov, A.: AERONET – A federated instrument network and data archive for aerosol characterization, Remote Sens. Environ., 66, 1–16, 1998.

Ichoku, C., Giglio, L., Wooster, M. J., and Remer, L. A.: Global characterization of biomass-burning patterns using satellite measurements of fire radiative energy, Remote Sens. Environ., 112, 2950–2962, 2008.

Kahn, R. A. and Limbacher, J.: Eyjafjallajökull volcano plume particle-type characterization from space-based multi-angle imaging, Atmos. Chem. Phys., 12, 9459–9477, doi:10.5194/acp-12-9459-2012, 2012.

Kahn, R., West, R., McDonald, D., Rheingans, B., and Mishchenko, M. I.: Sensitivity of multiangle remote sensing observations to aerosol sphericity, J. Geophys. Res.-Atmos., 102, 16861–16870, 1997.

Kahn, R., Banerjee, P., McDonald, D., and Diner, D. J.: Sensitivity of multiangle imaging to aerosol optical depth and to pure-particle size distribution and composition over ocean, J. Geophys. Res.-Atmos., 103, 32195–32213, 1998.

Kahn, R., Banerjee, P., and McDonald, D.: Sensitivity of multiangle imaging to natural mixtures of aerosols over ocean, J. Geophys. Res.-Atmos., 106, 18219–18238, 2001.

Kahn, R., Garay, M. J., Nelson, D. L., Yau, K. K., Bull, M. A., Gaitley, B. J., Martonchik, J. V., and Levy, R. C.: Satellite-derived aerosol optical depth over dark water from MISR and MODIS: Comparisons with AERONET and implications for climatological studies, J. Geophys. Res.-Atmos., 112, D18205, doi:10.1029/2006JD008175, 2007.

Kahn, R., Nelson, D., Garay, M., Levy, R., Bull, M., Diner, D., Martonchik, J. V., Paradise, S. R., Hansen, E. G., and Remer, L. A.: MISR Aerosol Product Attributes and Statistical Comparisons With MODIS, IEEE Trans. Geosci. Remote Sensing, 47, 4095–4114, 2009.

Kahn, R., Gaitley, B. J., Garay, M. J., Diner, D. J., Eck, T. F., Smirnov, A., and Holben, B. N.: Multiangle Imaging SpectroRadiometer global aerosol product assessment by comparison with the Aerosol Robotic Network, J. Geophys. Res.-Atmos., 115, D23209, doi:10.1029/2010JD014601, 2010.

Kalashnikova, O. V., Kahn, R., Sokolik, I. N., and Li, W. H.: Ability of multiangle remote sensing observations to identify and distinguish mineral dust types: Optical models and retrievals of optically thick plumes, J. Geophys. Res.-Atmos., 110, D18S14, doi:10.1029/2004JD004550, 2005.

Lee, K. H. and Kim, Y. J.: Satellite remote sensing of Asian aerosols: a case study of clean, polluted, and Asian dust storm days, Atmos. Meas. Tech., 3, 1771–1784, doi:10.5194/amt-3-1771-2010, 2010.

Levy, R. C., Mattoo, S., Munchak, L. A., Remer, L. A., Sayer, A. M., Patadia, F., and Hsu, N. C.: The Collection 6 MODIS aerosol products over land and ocean, Atmos. Meas. Tech., 6, 2989–3034, doi:10.5194/amt-6-2989-2013, 2013.

Li, C. C., Lau, A. K. H., Mao, J. T., and Chu, D. A.: Retrieval, validation, and application of the 1 km aerosol optical depth from MODIS measurements over Hong Kong, IEEE Trans. Geosci. Remote Sens., 43, 2650–2658, 2005a.

Li, Q. B., Jacob, D. J., Park, R., Wang, Y. X., Heald, C. L., Hudman, R., Yantosca, R. M., Martin, R. V., and Evans, M.: North American pollution outflow and the trapping of convectively lifted pollution by upper-level anticyclone, J. Geophys. Res.-Atmos., 110, D10301, doi:10.1029/2004JD005039, 2005b.

Li, S. S., Chen, L. F., Xiong, X. Z., Tao, J. H., Su, L., Han, D., and Liu, Y.: Retrieval of the Haze Optical Thickness in North China Plain Using MODIS Data, IEEE Trans. Geosci. Remote Sens., 51, 2528–2540, 2013.

Liu, Y., Sarnat, J. A., Coull, B. A., Koutrakis, P., and Jacob, D. J.: Validation of multiangle imaging spectroradiometer

(MISR) aerosol optical thickness measurements using aerosol robotic network (AERONET) observations over the contiguous United States, J. Geophys. Res.-Atmos., 109, D06205, doi:10.1029/2003JD003981, 2004.

Liu, Y., Koutrakis, P., and Kahn, R.: Estimating fine particulate matter component concentrations and size distributions using satellite-retrieved fractional aerosol optical depth: Part 1 – Method development, J. Air Waste Manage. Assoc., 57, 1351–1359, 2007a.

Liu, Y., Koutrakis, P., Kahn, R., Turquety, S., and Yantosca, R. M.: Estimating fine particulate matter component concentrations and size distributions using satellite-retrieved fractional aerosol optical depth: Part 2 - A case study, J. Air Waste Manage. Assoc., 57, 1360–1369, 2007b.

Liu, Y., Chen, D., Kahn, R. A., and He, K. B.: Review of the applications of Multiangle Imaging SpectroRadiometer to air quality research, Sci. China Ser. D-Earth Sci., 52, 132–144, 2009a.

Liu, Y., Kahn, R. A., Chaloulakou, A., and Koutrakis, P.: Analysis of the impact of the forest fires in August 2007 on air quality of Athens using multi-sensor aerosol remote sensing data, meteorology and surface observations, Atmos. Environ., 43, 3310–3318, 2009b.

Lohmann, U. and Lesins, G.: Stronger constraints on the anthropogenic indirect aerosol effect, Science, 298, 1012–1015, 2002.

Mahowald, N.: Aerosol Indirect Effect on Biogeochemical Cycles and Climate, Science, 334, 794–796, 2011.

Martin, R. V., Jacob, D. J., Yantosca, R. M., Chin, M., and Ginoux, P.: Global and regional decreases in tropospheric oxidants from photochemical effects of aerosols, J. Geophys. Res.-Atmos., 108, 4097, doi:10.1029/2002JD002622, 2003.

Martonchik, J. V., Kahn, R. A., and Diner, D. J.: Retrieval of Aerosol Properties over Land Using MISR Observations, in: Satellite Aerosol Remote Sensing Over Land, edited by: Kokhanovsky, A. A. and Leeuw, G. D., Springer, Berlin, 2009.

Myhre, G.: Consistency Between Satellite-Derived and Modeled Estimates of the Direct Aerosol Effect, Science, 325, 187–190, 2009.

Omar, A. H., Won, J. G., Winker, D. M., Yoon, S. C., Dubovik, O., and McCormick, M. P.: Development of global aerosol models using cluster analysis of Aerosol Robotic Network (AERONET) measurements, J. Geophys. Res.-Atmos., 110, D10S14, doi:10.1029/2004JD004874, 2005.

O'Neill, N. T., Ignatov, A., Holben, B. N., and Eck, T. F.: The lognormal distribution as a reference for reporting aerosol optical depth statistics; Empirical tests using multi-year, multi-site AERONET Sunphotometer data, Geophys. Res. Lett., 27, 3333–3336, 2000.

Reid, J. S., Eck, T. F., Christopher, S. A., Hobbs, P. V., and Holben, B.: Use of the Angstrom exponent to estimate the variability of optical and physical properties of aging smoke particles in Brazil, J. Geophys. Res.-Atmos., 104, 27473–27489, 1999.

Russell, P. B., Bergstrom, R. W., Shinozuka, Y., Clarke, A. D., De-Carlo, P. F., Jimenez, J. L., Livingston, J. M., Redemann, J., Dubovik, O., and Strawa, A.: Absorption Angstrom Exponent in AERONET and related data as an indicator of aerosol composition, Atmos. Chem. Phys., 10, 1155–1169, doi:10.5194/acp-10-1155-2010, 2010.

Stevens, B. and Feingold, G.: Untangling aerosol effects on clouds and precipitation in a buffered system, Nature, 461, 607–613, 2009.

van Donkelaar, A., Martin, R. V., Brauer, M., Kahn, R., Levy, R., Verduzco, C., and Villeneuve, P. J.: Global Estimates of Ambient Fine Particulate Matter Concentrations from Satellite-Based Aerosol Optical Depth: Development and Application, Environ. Health Perspect., 118, 847–855, 2010.

Wang, J., van den Heever, S. C., and Reid, J. S.: A conceptual model for the link between Central American biomass burning aerosols and severe weather over the south central United States, Environ. Res. Lett., 4, 015003, doi:10.1088/1748-9326/4/1/015003, 2009.

Wang, J., Xu, X. G., Spurr, R., Wang, Y. X., and Drury, E.: Improved algorithm for MODIS satellite retrievals of aerosol optical thickness over land in dusty atmosphere: Implications for air quality monitoring in China, Remote Sens. Environ., 114, 2575–2583, 2010.

Wang, J., Xu, X. G., Henze, D. K., Zeng, J., Ji, Q., Tsay, S. C., and Huang, J. P.: Top-down estimate of dust emissions through integration of MODIS and MISR aerosol retrievals with the GEOS-Chem adjoint model, Geophys. Res. Lett., 39, L08802, doi:10.1029/2012GL051136, 2012.

Yu, H. B., Remer, L. A., Chin, M., Bian, H. S., Tan, Q., Yuan, T. L., and Zhang, Y.: Aerosols from Overseas Rival Domestic Emissions over North America, Science, 337, 566–569, 2012.

Zhang, X. Y. and Kondragunta, S.: Temporal and spatial variability in biomass burned areas across the USA derived from the GOES fire product, Remote Sens. Environ., 112, 2886–2897, 2008.